NEOPLASIA
www.neoplasia.com

Volume 14 Number 6 June 2012 pp. 476–486 476

RB1 Methylation by SMYD2 Enhances Cell Cycle Progression through an Increase of RB1 Phosphorylation[1,2]

Hyun-Soo Cho[*,3], Shinya Hayami[*,†,3], Gouji Toyokawa[*,3], Kazuhiro Maejima[*], Yuka Yamane[*], Takehiro Suzuki[‡], Naoshi Dohmae[‡], Masaharu Kogure[*], Daechun Kang[*], David E. Neal[§], Bruce A.J. Ponder[§], Hiroki Yamaue[†], Yusuke Nakamura[*] and Ryuji Hamamoto[*,§]

*Laboratory of Molecular Medicine, Human Genome Center, Institute of Medical Science, The University of Tokyo, Tokyo, Japan; [†]Second Department of Surgery, School of Medicine, Wakayama Medical University, Wakayama, Japan; [‡]Biomolecular Characterization Team, RIKEN, Saitama, Japan; [§]Department of Oncology, Cancer Research UK Cambridge Research Institute, University of Cambridge, Cambridge, UK

Abstract

It is well known that RB functions are regulated by posttranslational modifications such as phosphorylation and acetylation, but the significance of lysine methylation on RB has not been fully elucidated. Our expression analysis of *SMYD2* by quantitative real-time polymerase chain reaction showed that expression levels of *SMYD2* are significantly elevated in human bladder carcinomas compared with nonneoplastic bladder tissues ($P < .0001$), and its expression levels in tumor tissues were much higher than those of any other normal tissues. SMYD2 knockdown resulted in the suppression of cancer cell growth, and cell cycle analysis indicated that SMYD2 might play a crucial role in the G_1/S transition. According to an *in vitro* methyltransferase assay, we found that SMYD2 methylates RB1 protein, and liquid chromatography–tandem mass spectrometry analysis revealed lysine 810 of RB1 to be methylated by SMYD2. Importantly, this methylation enhanced Ser 807/811 phosphorylation of RB1 both *in vitro* and *in vivo*. Furthermore, we demonstrated that methylated RB1 accelerates E2F transcriptional activity and promotes cell cycle progression. SMYD2 is an important oncoprotein in various types of cancer, and SMYD2-dependent RB1 methylation at lysine 810 promotes cell cycle progression of cancer cells. Further study may explore SMYD2-dependent RB1 methylation as a potential therapeutic target in human cancer.

Neoplasia (2012) 14, 476–486

Introduction

The retinoblastoma tumor suppressor protein (RB) has a central role in cell cycle regulation and is mutated in several types of cancer [1–3]. RB can interact with the E2F transcription factor and regulate genes related to S-phase entry. In its hypophosphorylated state RB binds to E2F and repress the expression of E2F target genes. When RB is hyperphosphorylated by the Cyclin/CDK complexes, E2F is separated from RB and transactivates its target genes that drive cell cycle progression [1,2,4,5]. Although *RB* has been reported to be inactivated in more than 90% of human small cell lung carcinomas [1], most human cancers express wild-type RB that is predominantly at a phosphorylated state because of the deregulation of CDKs. Thereby, most human

Address all correspondence to: Dr. Ryuji Hamamoto, Laboratory of Molecular Medicine, Human Genome Center, Institute of Medical Science, The University of Tokyo, 4-6-1 Shirokanedai, Minato-ku, Tokyo 108-8639, Japan. E-mail: ryuji@ims.u-tokyo.ac.jp

[1]This work was supported by a Grant-in-Aid for Young Scientists (A) (22681030) from the Japan Society for the Promotion of Science. Y.Y. and K.M. are employees of OncoTherapy Science, Inc. R.H. is a scientific advisor of OncoTherapy Science, Inc.
[2]This article refers to supplementary materials, which are designated by Tables W1 to W2 and Figures W1 to W6 and are available online at www.neoplasia.com.
[3]Both authors contributed equally to this work.
Received 10 April 2012; Revised 5 May 2012; Accepted 7 May 2012

DOI 10.1593/neo.12656

cancers seem to have lost the G_1 checkpoint control through the deregulation of RB functions, and phosphorylation of RB is the key regulatory step in the pathway controlling proliferation of cancer cells [2]. In addition to phosphorylation, RB protein has been known to be acetylated [6,7]. During keratinocyte differentiation, RB is acetylated by the acetyltransferase P-CAF, and the acetylation of two major lysine residues (lysines 873 and 874) that are located within the nuclear localization signal is likely to play a crucial role in differentiation through the retention of the RB protein in the nucleus [8]. However, the significance of other posttranslational modifications including lysine methylation for regulation of RB functions still remains unclear.

SMYD2 was first identified as one of the SMYD family members, containing a SET domain and a MYND domain [9]. SMYD2 methylates H3K36 and functions as a transcriptional regulator in cooperation with the Sin3A and HDAC1 histone deacetylase complex [9]. Besides histone methylation process, SMYD2 also methylates p53 and altering their functions [10]. In *Xenopus laevis*, smyd2 is expressed in muscle tissues and might be associated with muscle cells differentiation [11]. In addition, Diehl et al. [12] showed that Smyd2 is expressed in various types of neonatal mouse tissues and particularly neonatal heart. However, Smyd2 is not critical for mouse heart development, unlike Smyd1, which is indispensable for cardiomyocyte differentiation and cardiac morphogenesis [13]. Thus, although a part of biologic functions have been clarified, the roles of SMYD2 in both nonneonatal cellular biology and diseases like cancer remains largely unclear.

In this study, we show evidences that SMYD2 methylates lysine 810 of RB1, elevates phsophorylation level of RB, and promotes the cell cycle progression. Our findings demonstrate a novel posttranslational modification of RB1, which may play a critical role in human carcinogenesis.

Materials and Methods

Bladder Tissue Samples and RNA Preparation

Bladder tissue samples and RNA preparation were described previously [14–20]. Briefly, 125 surgical specimens of primary urothelial carcinoma were collected, either at cystectomy or at transurethral resection of bladder tumor (TURBT), and snap-frozen in liquid nitrogen. Twenty-eight specimens of normal bladder urothelial tissue were collected from areas of macroscopically normal bladder urothelium in patients with no evidence of malignancy. Vimentin is primarily expressed in mesenchymally derived cells, and it was used as a stromal marker. Uroplakin is a marker of urothelial differentiation and is preserved in up to 90% of epithelially derived tumors [21]. Use of tissues for this study was approved by Cambridgeshire Local Research Ethics Committee (reference no. 03/018). RNA samples of normal tissues (brain, breast, colon, esophagus, eye, heart, liver, lung, pancreas, placenta, kidney, rectum, spleen, stomach and testis) were purchased from BioChain (Newark, CA).

Cell Lines

CCD-18Co, HFL1, 5637, SW780, SCaBER, UMUC3, RT4, T24, HT-1197, HT-1376, A549, H2170, SW480, HCT116, LoVo, COS7, HeLa, and 293T cells were from the American Type Culture Collection (Manassas, VA) in 2001 and 2003 and tested and authenticated by DNA profiling for polymorphic short tandem repeat (STR) markers except for SW780. The SW780 line was established in 1974 by A. Leibovitz from a grade 1 transitional cell carcinoma. RERF-LC-AI and SBC5 cells were from the Japanese Collection of Research Bioresources (Osaka, Japan) in 2001 and tested and authenticated by DNA profiling for polymorphic STR markers. 253J, 253J-BV, and SNU-475 cells were from the Korean Cell Line Bank (Seoul, Korea) in 2001 and tested and authenticated by DNA profiling for polymorphic STR markers. EJ28 cells were from Cell Lines Service (Eppelheim, Germany) in 2003 and tested and authenticated by DNA profiling for polymorphic STR markers. ACC-LC-319 cells were from Aichi Cancer Center (Nagoya, Japan) in 2003 and tested and authenticated by DNA profiling for SNP, mutation, and deletion analysis.

All cell lines were grown in monolayers in appropriate media: Dulbecco modified Eagle medium (DMEM) for EJ28, RERF-LC-AI, COS-7, and 293T cells; Eagle minimum essential medium for CCD-18Co, WI-38, 253J, 253J-BV, HT-1376, SCaBER, UMUC3, HeLa and SBC5 cells; Leibovitz L-15 for SW480 and SW780 cells; McCoy 5A medium for RT4, T24, and HCT116 cells; RPMI 1640 medium for 5637, A549, H2170, ACC-LC-319, and SNU-475 cells. LoVo cells were cultured in Ham F-12 medium supplemented with 20% fetal bovine serum (FBS) and 1% antibiotic/antimycotic solution (Sigma-Aldrich, St Louis, MO). All cells were maintained at 37°C in humid air with 5% CO_2 condition (SAEC, 5637, 253J, 253J-BV, EJ28, HT-1197, HT-1376, J82, RT4, SCaBER, T24, UMUC3, A549, H2170, ACC-LC-319, RERF-LC-AI, SBC5, and 293T cells) or without CO_2 (SW480 and SW780 cells). Cells were transfected with FuGENE 6 (Roche Applied Science, Penzberg, Germany) according to the manufacturer's protocols.

Quantitative Real-time Polymerase Chain Reaction

As described above, we prepared 125 bladder cancer and 28 normal bladder tissues in Addenbrooke's Hospital, Cambridge. For quantitative real-time polymerase chain reactions (RT-PCRs), specific primers for all human *GAPDH* (housekeeping gene), *SDH* (housekeeping gene), and *SMYD2* were designed (primer sequences in Table W1). PCRs were performed using the LightCycler 480 System (Roche Applied Science) following the manufacturer's protocol.

Immunohistochemical Staining

Paraffin-embedded tissue slides were purchased from BioChain. Immunohistochemistry was performed using VECTASTAIN ABC Reagent (PK-7100; Vector Laboratories, Burlingame, CA) and DAB substrate kit for peroxidase (SK-4100; Vector Laboratories). Slides of paraffin-embedded bladder tumor specimens and normal human tissues were deparaffinized in xylene and followed by rehydration in 99% ethanol. After wash by 1 × PBS (–), the slides were processed under high pressure (125°C for 30 seconds) in an antigen retrieval solution, high pH 9 (S2367; Dako, Carpinteria, CA), and quenching was performed by 0.3% hydrogen peroxide (H_2O_2) in methanol for 15 minutes. After blocking by 3% bovine serum albumin, tissue sections were incubated overnight with a goat anti-SMYD2 polyclonal antibody (sc-79084; Santa Cruz Biotechnology, Santa Cruz, CA) at a 1:250 dilution ratio, followed by reaction with an antigoat biotinylated IgG for 1 hour. After incubation with Vectastain ABC reagent, color developing was performed using DAB substrate kit for peroxidase. Finally, tissue specimens were stained with Mayer hematoxylin (Hematoxylin QS; Vector Laboratories) to discriminate the nucleus from the cytoplasm.

Small interfering RNA Transfection

siRNA oligonucleotide duplexes were purchased from Sigma-Aldrich for targeting the human *SMYD2* transcripts. siNegative

control (siNC), which is a mixture of three different oligonucleotide duplexes, was used as control siRNAs. The siRNA sequences are described in Table W2. siRNA duplexes (final concentration, 100 nM) were transfected into bladder and lung cancer cell lines with Lipofectamine 2000 (Life Technologies, Carlsbad, CA) [17,22].

Clonogenicity Assays

COS-7 cells, cultured in DMEM 10% FBS, were transfected with a p3×FLAG-Mock, p3×FLAG-SMYD2 wild-type (WT), or a p3×FLAG-SMYD2 enzyme-dead mutant vector (ΔNHSC/ΔGEEV). The transfected COS-7 cells were cultured for 2 days and seeded in a 10-cm dish at the density of 10,000 cells per 10-cm dish in triplicate. Subsequently, the cells were cultured in DMEM 10% FBS containing 0.4 (mg/ml) Geneticin/G-418 for 2 weeks until colonies were visible. Colonies were stained with Giemsa (Merck, Whitehouse Station, NJ) and counted by Colony Counter software (Vector, Tokyo, Japan).

Mass Spectrometry

A protein band of SDS–polyacrylamide gel electrophoresis was excised and reduced with dithiothreitol and carboxymethylated by iodoacetic acid. After washing the gel, the band was digested with Achromobacter Protease I (API, Lys-C a gift from Dr Masaki, Ibaraki University) at 37°C overnight [23]. An aliquot of digest was analyzed by nano liquid chromatography–tandem mass spectrometry (LC-MS/MS) using LCQ Deca XP plus (Thermo Fisher Scientific, San Jose, CA). The peptides were separated using nano ESI spray column (100 μm [ID] × 50 mm [L]) packed with a reversed-phase material (Inertsil ODS-3, 3 μm; GL Science, Tokyo, Japan) at a flow rate 200 nl/min. The mass spectrometer was operated in the positive-ion mode, and the spectra were acquired in a data-dependent MS/MS mode. The MS/MS spectra were searched against the in-house database using local MASCOT server (version 2.2.1; Matrix Sciences, London, United Kingdom). The reduced and carboxylmethyated gel band was also digested with endoproteinase Asp-N (Roche Applied Science) at 37°C overnight. An aliquot of digest was deslated and applied to MALDI-TOF-MS using an Ultraflex (Bruker Daltonik GmbH, Bremen, Germany). And a selected peak was analyzed matrix-assisted laser desorption/ionization tandem time-of-flight (MALDI-TOF/TOF) tandem mass spectrometry in a LIFT mode.

Amino Acid Analysis

The excised protein bands blotted on the polyvinylidene fluoride membrane were individually inserted in clean 6 × 32-mm glass tubes containing 50 pmol of norvaline as internal standard and hydrolyzed in 6N HCl vapor at 110°C for 20 hours. The hydrolyzed samples were derivatized *in situ* by 6-aminoquinolyl-*N*-hydroxysuccinimidyl carbamate for fluorophore detection. The 6-aminoquinolyl-*N*-hydroxysuccinimidyl carbamate amino acids were separated by ion-pair chromatography on a C18 reversed-phase column (Inertsil ODS-3, 4.6 mm [ID] × 150 mm, 3 μm; GL Sciences, Tokyo, Japan). Both a laser-induced fluorescence detector (LIF726; GL Sciences) and a fluorescence detector with Xe flush lamp (G1312A; Agilent Technologies, Santa Clara, CA) were used to reveal the existence of monomethylated Lys [24].

Immunocytochemistry

Cells were fixed with PBS (–) containing 4% paraformaldehyde for 30 minutes, and rendered permeable with PBS (–) containing 0.1% Triton X-100 at room temperature for 2 minutes. Subsequently, the cells were covered with PBS (–) containing 3% bovine serum albumin for 1 hour at room temperature to block nonspecific hybridization and were then incubated with rabbit anti-Rb (sc-102; Santa Cruz Biotechnology), anti-p-Rb (Ser 807/811)-R (sc-16670-R; Santa Cruz Biotechnology), goat anti-SMYD2 (sc-79084; Santa Cruz Biotechnology), and mouse anti-FLAG (Sigma-Aldrich) at a 1:500 dilution ratio. After washing with PBS (–), cells were stained by an Alexa Fluor 488–conjugated antirabbit secondary antibody (Life Technologies) or an Alexa Fluor 594–conjugated antimouse secondary antibody (Life Technologies) at a 1:500 dilution ratio. Nuclei were counterstained with 4′,6′-diamidine-2′-phenylindole dihydrochloride (DAPI). Fluorescent images were obtained under a TCS SP2 AOBS microscope (Leica Microsystems, Wetzlar, Germany).

Immunoprecipitation

293T cells were seeded at a density of 5×10^5 cells on a 100-mm dish. The next day, the cells were transfected with expression vector constructs using FuGENE 6 (Roche Applied Science) according to the manufacturer's recommendation. After 48 hours, transfected 293T cells were washed with PBS and lysed in CelLytic M Cell Lysis Reagent (Sigma-Aldrich) containing complete protease inhibitor cocktail (Roche Applied Science). Five hundred micrograms of whole-cell extract was incubated with anti-FLAG M2 agarose (Sigma-Aldrich) for 1 hour at 4°C. After the beads were washed three times with 1 ml of TBS buffer (pH 7.6), the FLAG-tagged proteins bound to the beads were eluted by boiling in Lane Marker Sample Buffer (Thermo Fisher Scientific, Hudson, NH). Samples were then subjected to SDS-PAGE and detected by silver staining or Western blot.

Western Blot

Whole-cell lysates were prepared from the cells with RIPA-like buffer or CelLytic M Cell Lysis Reagent (Sigma-Aldrich) containing complete protease inhibitor cocktail (Roche Applied Science) and total protein or immunoprecipitated samples were transferred to nitrocellulose membrane. The membrane was probed with anti-SMYD2 (sc-79084; Santa Cruz Biotechnology), anti-Rb (sc-102; Santa Cruz Biotechnology), anti–phospho-Rb (Ser 807/811)-R (sc-16670-R; Santa Cruz Biotechnology), anti–phospho-Rb (Ser 780) (C84F6; Cell Signaling Technology, Danvers, MA), anti-ACTB (I-19, Santa Cruz Biotechnology), anti-FLAG (Sigma-Aldrich), anti-HA (Santa Cruz Biotechnology), and anti-His (631212; Clontech Laboratories, Mountain View, CA) antibodies. An anti–mono-methylated RB1 K810 antibody was made by Sigma-Aldrich. Protein bands were detected by MemCode Reversible Protein Stain Kit (24580; Thermo Fisher Scientific).

In Vitro *Methyltransferase Assay*

For the *in vitro* methylation assay, His-WT-RB1, His-K810A-RB1, and His-SMYD2 were used as described previously. One microgram of RB1 was incubated with 1 μg of SMYD2 in 1.0 M Tris-HCl (pH 8.8), 1.0 μCi/ml *S*-adenosyl-L-[methyl-^{3}H] methionine (SAM; Perkin Elmer, Waltham, MA) and Milli-Q water for 1 hour at 30°C. After boiling in sample buffer, the samples were subjected to SDS-PAGE, followed by visualization by fluorography [25].

In Vitro *Kinase Assay*

CDK4/Cyclin D1 (ab55695; Abcam, Cambridge, United Kingdom) was used for kinase assay in a reaction buffer containing 40 mM MOPS (pH 7.0), 1 mM EDTA, and 20 mM ATP for 10 minutes at 30°C. After boiling in sample buffer, the samples were subjected to SDS-PAGE.

Results

SMYD2 Is Overexpressed in Human Cancer and Regulates the Growth of Cancer Cells

We examined expression levels of genes belonging to the histone methyltransferase family in clinical bladder samples and found a significant increase in the SMYD2 expression compared with normal bladder epithelial cells. Then we analyzed 125 bladder cancer samples and 28 normal control samples (British) and confirmed significant elevation of *SMYD2* expression in tumor cells ($P < .0001$, Mann-Whitney U test) (Figure 1*A* and Table 1, patient characteristics). We also compared the expression levels of *SMYD2* between bladder tumor and various types of normal tissues and found that the expression of *SMYD2* in bladder tumor tissues is significantly higher than those in normal tissues, including the heart, the lung, the liver, and the kidney (Figure 1*B*). Immunohistochemical analysis using an anti-SMYD2 antibody confirmed overexpression of SMYD2 at the protein level in bladder cancer tissue sections (Figure 1*C*).

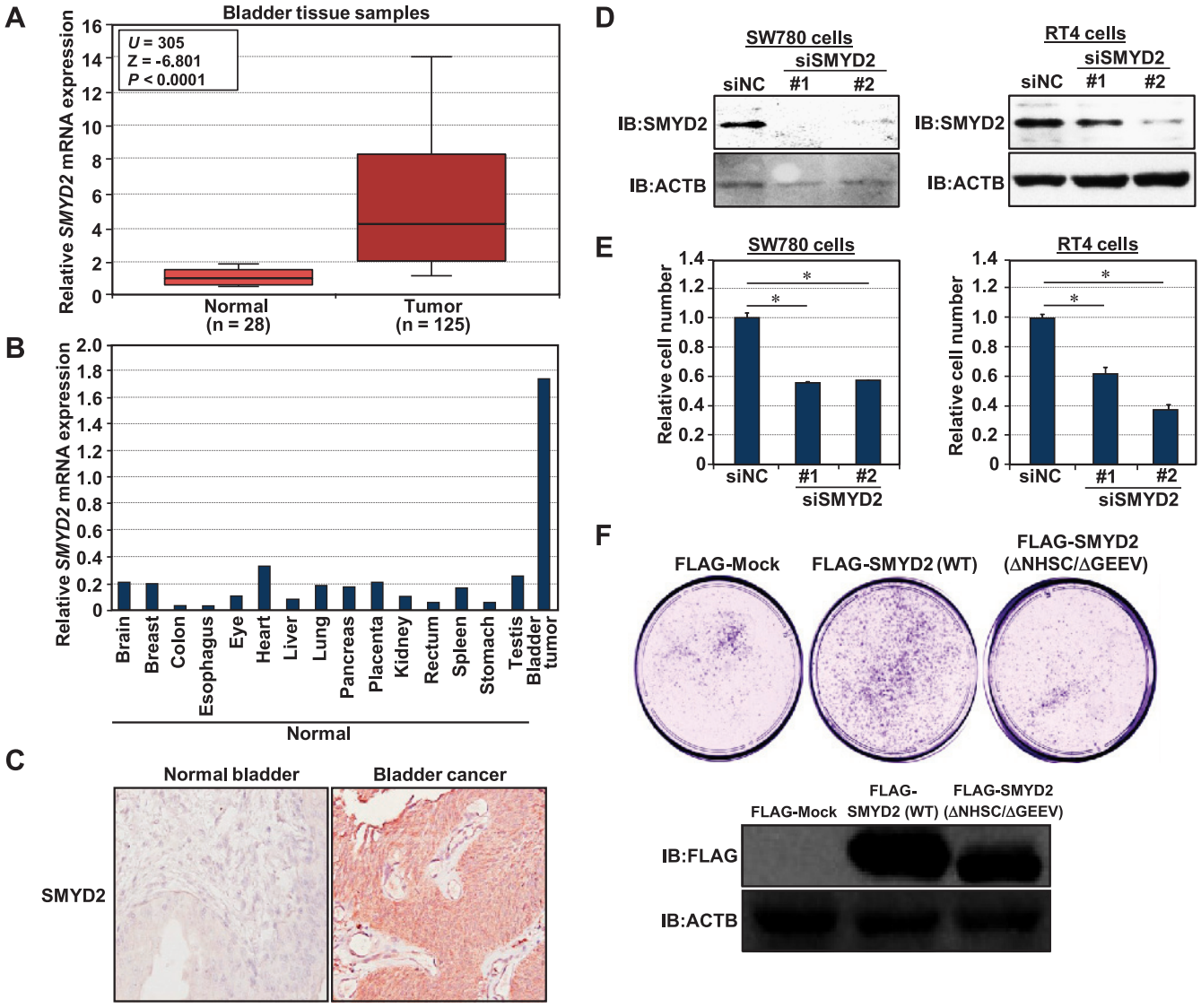

Figure 1. SMYD2 is overexpressed in cancer tissues and involved in the growth of cancer cells. (A) Expression analysis of *SMYD2* at mRNA levels in 125 bladder cancer cases and 28 normal bladder cases by quantitative RT-PCR, and results are shown by box-whisker plot. *GAPDH* and *SDH* were used as housekeeping genes. Mann-Whitney U test was used for statistical analysis ($P < .0001$). (B) Comparison of mRNA levels of SMYD2 between bladder cancer samples and normal organ tissues. The normal organ tissues include brain, breast, colon, esophagus, eye, heart, liver, lung, pancreas, placenta, kidney, rectum, spleen, stomach, and testis. (C) Immunohistochemical analysis of bladder cancer and normal bladder tissues. All tissue samples were purchased from BioChain. Original magnification, ×200. (D) Validation of SMYD2 knockdown at the protein level. Lysates from SW780 and RT4 cells 72 hours after siRNA treatment were immunoblotted with anti-SMYD2 and anti-ACTB (an internal control) antibodies. (E) Effects of SMYD2 knockdown on the proliferation of bladder cancer cell lines (SW780 and RT4) measured by Cell Counting Kit-8. Relative cell numbers are normalized to the number of siNC-treated cells (siNC = 1): results are the mean ± SD (error bars) of three independent experiments. P values were calculated using Student's t test (*, $P < .05$). (F) Methylation activity of SMYD2 is critical for its growth-promoting effect. COS-7 cells were transfected with FLAG-Mock, -SMYD2 (WT or ΔNHSC/ΔGEEV) and, 10 days after transfection, were stained with Giemsa. Expression of SMYD2 (WT or ΔNHSC/ΔGEEV) was confirmed by Western blot using anti-FLAG antibody. Expression of ACTB served as a control.

Table 1. Statistical Analysis of *SMYD2* Expression Levels in Clinical Bladder Tissues.

Characteristic	*n*	SMYD2		
		Mean	SD	95% CI
Normal (control)	28	1.055	0.512	0.866-1.245
Tumor (total)	125	7.092	10.474	5.256-8.929
Tumor grade				
1	12	6.879	4.391	4.395-9.363
2	63	8.633	13.833	5.217-12.049
3	49	5.195	5.001	3.794-6.595
Metastasis				
Negative	98	7.442	11.551	5.155-9.729
Positive	27	5.823	4.831	4.001-7.646
Sex				
Male	91	6.623	8.600	4.856-8.390
Female	32	5.210	5.120	3.436-6.984
Recurrence				
No	28	9.221	13.198	4.332-14.110
Yes	51	5.541	5.465	4.041-7.041
Died	8	5.539	6.733	0.873-10.205
Smoke				
No	27	5.882	4.601	4.147-7.618
Yes	49	7.476	11.231	4.331-10.620

CI indicates confidence interval.

Furthermore, the Oncomine database records that SMYD2 is overexpressed in various types of human cancer: colon, prostate, and breast cancer (Figure W1). These results indicate that expression levels of SMYD2 are widely elevated in human cancer.

To investigate whether SMYD2 is indispensable for cancer cell viability, we first examined expression levels of SMYD2 in cell lines and found overexpression of SMYD2 in bladder, lung, colon, and liver cancer cell lines compared with the normal fibroblast cell line WI-38 (Figure W2). We then suppressed the *SMYD2* expression in bladder cancer cells (SW780 and RT4) using two independent siRNAs. After confirming knockdown by those siRNAs (Figure 1*D*), we performed cell growth assays and found significant growth suppression of the cells treated with SMYD2 siRNAs compared with control siRNA (siNC; Figure 1*E*). Significant growth suppression was also observed when we used lung cancer cell lines (A549, ACC-LC-319, and SBC5; Figure W3). To examine oncogenic activity of SMYD2, we conducted a clonogenicity assay. We transfected either a wild-type SMYD2 (SMYD2 WT) vector, an enzyme-dead SMYD2 (SMYD2 ΔNHSC/ΔGEEV) vector, or a mock vector into COS-7 cells and performed a clonogenicity assay (Figure 1*F*). The cells transfected with a wild-type SMYD2 vector were found to form more colonies than those transfected with an enzyme-dead SMYD2 vector or a mock control vector, implying the importance of the methylation activity of SMYD2 in its oncogenic activity. Because overexpression of SMYD2 was observed in an early-stage cancer, SMYD2 may play a crucial role in an early step of carcinogenesis.

To further elucidate the biologic effects of SMYD2 on the growth of cancer cells, we introduced a SMYD2 expression vector containing the Flp-In T-REx system (T-REx-293; Life Technologies) into human embryonic kidney fibroblast (HEK293) cells. We transfected either a V5-tagged SMYD2 expression vector (SMYD2), an empty vector (Control), or a V5-tagged CAT expression vector (CAT) into T-REx-293 cells and then established cell lines overexpressing SMYD2. We analyzed cell cycle status by FACS analysis (Figure W4*A*) and found that the proportion of cells in the S phase in those overexpressing SMYD2 was significantly increased compared with control ($P < .01$) or CAT ($P < .05$). Concordantly, the proportion of cells in the G_0/G_1 phase in those overexpressing SMYD2 was slightly lower than in the two control cells ($P < .01$ [Mock, SMYD2] and $P < .01$ [CAT, SMYD2], respectively). We also performed BrdU and 7-amino-actinomycin D staining to analyze the detailed cell cycle status of cancer cells and confirmed that the proportion of cancer cells at the S phase was significantly decreased after the knockdown of SMYD2 (Figure W4*B*).

SMYD2 Methylates Lysine 810 of RB1 Both In Vitro *and* In Vivo

To identify a critical substrate of SMYD2 involved in human carcinogenesis, we performed an *in vitro* methyltransferase assay using various tumor-related proteins as substrates and found a strong methylation signal when we used RB1 protein as a substrate (Figure 2*A*). To further verify the interaction between RB1 and SMYD2 proteins, we carried out a coimmunoprecipitation assay after cotransfection of FLAG-SMYD2 and HA-RB1 or FLAG-RB1 and HA-SMYD2 expression vectors into 293T cells and confirmed their bindings (Figure 2, *B* and *C*). In addition, an immunoprecipitation assay using deletion mutants of SMYD2 showed that the C-terminal portion of SMYD2 is essential to interact with RB1 (Figure 2*D*). Furthermore, we also confirmed the colocalization of endogenous RB1 and SMYD2 proteins in the small cell lung cancer cell line SBC5 by immunocytochemical analysis (Figure 2*E*).

We next constructed plasmid vectors that were designed to express parts of RB1 protein to identify a methylation site of RB1 by SMYD2 and prepared recombinant proteins expressed in *Escherichia coli*. Using those proteins, we conducted an *in vitro* methyltransferase assay (Figure 3*A*) and found that the C-terminal region (773 aa to 928 aa) of RB1 protein includes the methylation site(s). Subsequent LC-MS/MS analysis indicated lysine 810 on RB1 to be monomethylated by SMYD2 (Figure 3*B*). The SMYD2-dependent lysine monomethylation was also confirmed by amino acid analysis (Figure W5). To validate the methylation site of RB1 we identified, we prepared a partial RB1 protein, which was replaced lysine 810 to alanine (K810A-RB1 (773-813)) and performed an *in vitro* methyltransferase assay (Figure 3*C*). The specific methylation signal of the wild-type RB1 protein by SMYD2 was by the replacement of K810. On the basis of these results, we generated a polyclonal antibody targeting K810-monomethylated RB1 peptide. To validate the specificity of the antibody, we performed an *in vitro* methyltransferase assay with or without SMYD2 and observed a SMYD2-dependent methylation signal (Figure 3*D*). We also found that this antibody could recognize neither the K810-substituted RB1 protein treated with wild-type SMYD2 *in vitro* (Figure 3*E*) nor the wild-type RB1 protein treated with enzyme-dead SMYD2 *in vivo* (Figure 3*F*). These results imply that SMYD2 methylates lysine 810 of RB1 protein both *in vitro* and *in vivo*, and the antibody we generated can specifically recognize K810-methylated RB1.

SMYD2 Enhances Phosphorylation of RB1 at Ser 807/811 through Methylation of Lys 810

As it is well known that phosphorylation plays a crucial role in the regulation of RB1 functions [3,5], we examine the effect of Lys 810 methylation on the phosphorylation status of RB1. We first performed Western blot analysis of two noncancerous cell lines and seven cancer cell lines to examine the phosphorylation status of RB1 at Ser 807/811 and found some correlation between the higher phosphorylation status of RB1 and high SMYD2 expression (Figure 4*A*). To clarify whether SMYD2 affects RB1 phosphorylation status through methylation of Lys 810, we conducted gain-of-function and loss-of-function

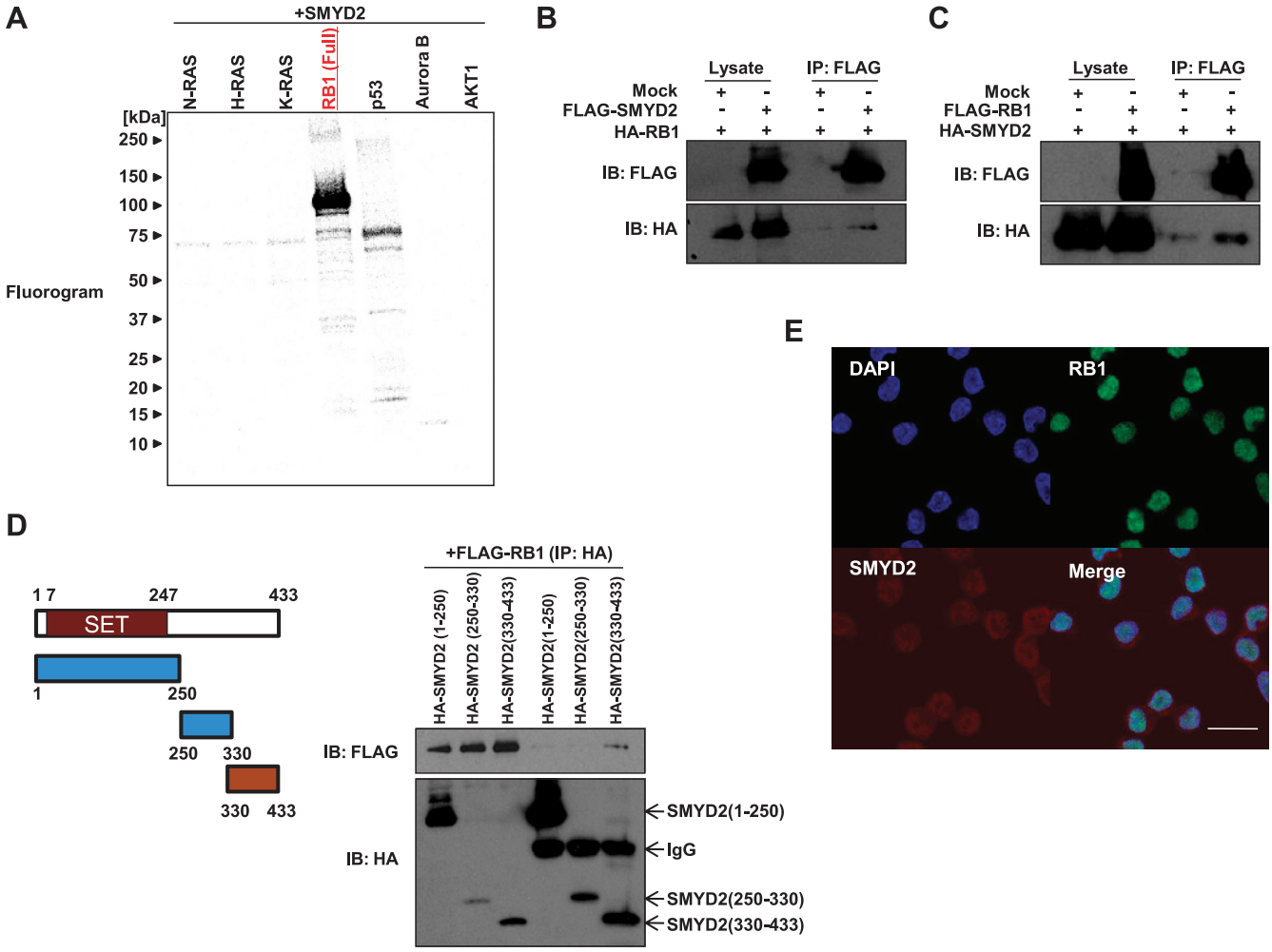

Figure 2. SMYD2 methylates RB1 and makes a complex through its C-terminal domain. (A) RB1 is methylated by SMYD2. *In vitro* methyltransferase reaction was performed using purified N-RAS, H-RAS, K-RAS, RB1, p53, Aurora B, and AKT1 recombinant proteins. Methylated proteins were visualized with fluorography. (B and C) Coimmunoprecipitation assays of SMYD2 and RB1 proteins. 293T cells were cotransfected with a SMYD2 expression vector and a RB1 expression vector or a mock control vector. The interaction of FLAG-SMYD2 and HA-RB1 (B) or FLAG-RB1 and HA-SMYD2 (C) was examined by immunoprecipitation using anti-FLAG M2 agarose and immunoblotted with anti-FLAG and anti-HA antibodies. (D) The C-terminal region of SMYD2 is essential for the interaction with RB1. 293T cells were cotransfected with a FLAG-RB1 expression vector and three different regions of HA-SMYD2 vectors (amino acids 1-250, 250-330, and 320-433 in SMYD2 protein). Immunoprecipitation was performed using HA-Agarose, and samples were immunoblotted with anti-FLAG and -HA antibodies. (E) Colocalization of SMYD2 and RB1 proteins in SBC5 cells. SBC5 cells were stained with anti-RB1 (Alexa Fluor 488 [green]) and anti-SMYD2 (Alexa Fluor 594 [red]) antibodies, and DAPI [blue]). Scale bar, 30 μm.

experiments. After introduction of FLAG-SMYD2 into 293T cells, we detected a significant elevation of phosphorylation status of RB1 at Ser 807/811 compared with the cells transfected with a mock vector (Figure 4*B*). Subsequent immunocytochemical analysis detected that overexpression of WT-SMYD2 enhanced phosphorylation of RB1 at Ser 807/811 in HeLa cells (Figure 4*C*). Concordantly, phosphorylation of RB1 at Ser 807/811 was significantly reduced after knockdown of SMYD2 (Figure 4*D*). To examine the effect of methyltransferase activity of SMYD2 on phosphorylation status of RB1, we transfected a vector designed to express a partial RB1 (FLAG-RB1(773-813)) together with a wild-type SMYD2 expression vector (HA-SMYD2) or with an enzyme-dead SMYD2 expression vector (HA-SMYD2 (ΔNHSC/GEEV)) into 293T cells, and conducted immunoprecipitation using anti-FLAG M2 agarose. As shown in Figure 4*E*, the phosphorylation level of RB1 at Ser 807/811 in the cells transfected with WT-SMYD2 was significantly higher than that in the cells with enzyme-dead SMYD2. Hence, SMYD2-dependent RB1 methylation seems to enhance phosphorylation status of RB1 at Ser 807/811.

To evaluate the effect of SMYD2-dependent methylation on the phosphorylation status of RB1, we performed an *in vitro* kinase assay using RB1 as a substrate reacted with or without SMYD2 (Figure 5*A*). After confirmation of Lys 810 methylation of RB1 (Figure 5*B*, *top*), we reacted the samples with the CDK4/Cyclin D1 complex, which is an important regulator of RB1 phosphorylation, and monitored phosphorylation status of RB1 at Ser 807/811 by Western blot (Figure 5*B*, *bottom*). Importantly, methylated RB1 showed higher phosphorylation levels than nonmethylated protein. In addition, when we examined the dose-dependent effect of SMYD2 on the RB1 phosphorylation at Ser 807/811, it was increased in a dose-dependent manner, correlating with methylation levels of RB1 at Lys 810 (Figure 5*C*). Likewise,

mutant RB1 containing a substitution of Lys 810 to alanine showed much weaker phosphorylation levels than wild-type RB1 (Figure 5*D*), implying that methylation of RB1 at Lys 810 seems to enhance phosphorylation levels of RB1. We then prepared a K810 monomethylated RB1 peptide (K810me-RB1 peptide) and a K810 unmethylated RB1 peptide (Control-RB1 peptide) and investigated the effect of K810 monomethylation on the phosphorylation of RB1 at Ser 807/811 by the CDK4/Cyclin D1 complex in more detail (Figure 5*E*). After confirmation of K810 monomethylation by dot blot analysis using an anti-RB1 K810me antibody, we conducted a kinase assay and found significantly higher phosphorylation levels of RB1 at Ser 807/811 in the K810me-RB1 peptide than in the unmethylated peptides (Figure 5*F*). The CDK4 dose-dependent elevation of RB1 phosphorylation at Ser 807/811 in the K810me-RB1 was also confirmed (Figure 5*G*). These findings indicate that K810 monomethylation of RB1 by SMYD2 can enhance the phosphorylation level of RB1 at Ser 807/811.

Lys 810 Methylation of RB1 Promotes Cell Cycle Progression

To further evaluate the effect of methylation on phosphorylation status of RB1 *in vivo*, we transfected a FLAG-WT-RB1 vector or a FLAG-K810A-RB1 vector with a HA-WT-SMYD2 vector into 293T cells and carried out immunoprecipitation with anti-FLAG M2 agarose (Figure 6*A*). Consistent with previous data, WT-RB1 showed higher phosphorylation levels of RB1 at Ser 807/811 than Lys 810–substituted RB1 (K810A-RB1), and this result was also confirmed using a partial RB1 (773-813) (Figure 6*B*). Taken together, methylation of RB1 at Lys 810 also seems to enhance the phosphorylation status of RB1 *in vivo*.

It is known that CDK-mediated phosphorylation of RB1 prevents the interaction of RB1 with E2F1, a multifunctional transcription factor that activates the genes required for the cell cycle progression at the G_1/S transition and enables E2F1-dependent gene expression [5]. Because Lys 810 methylation enhanced the phosphorylation of RB1,

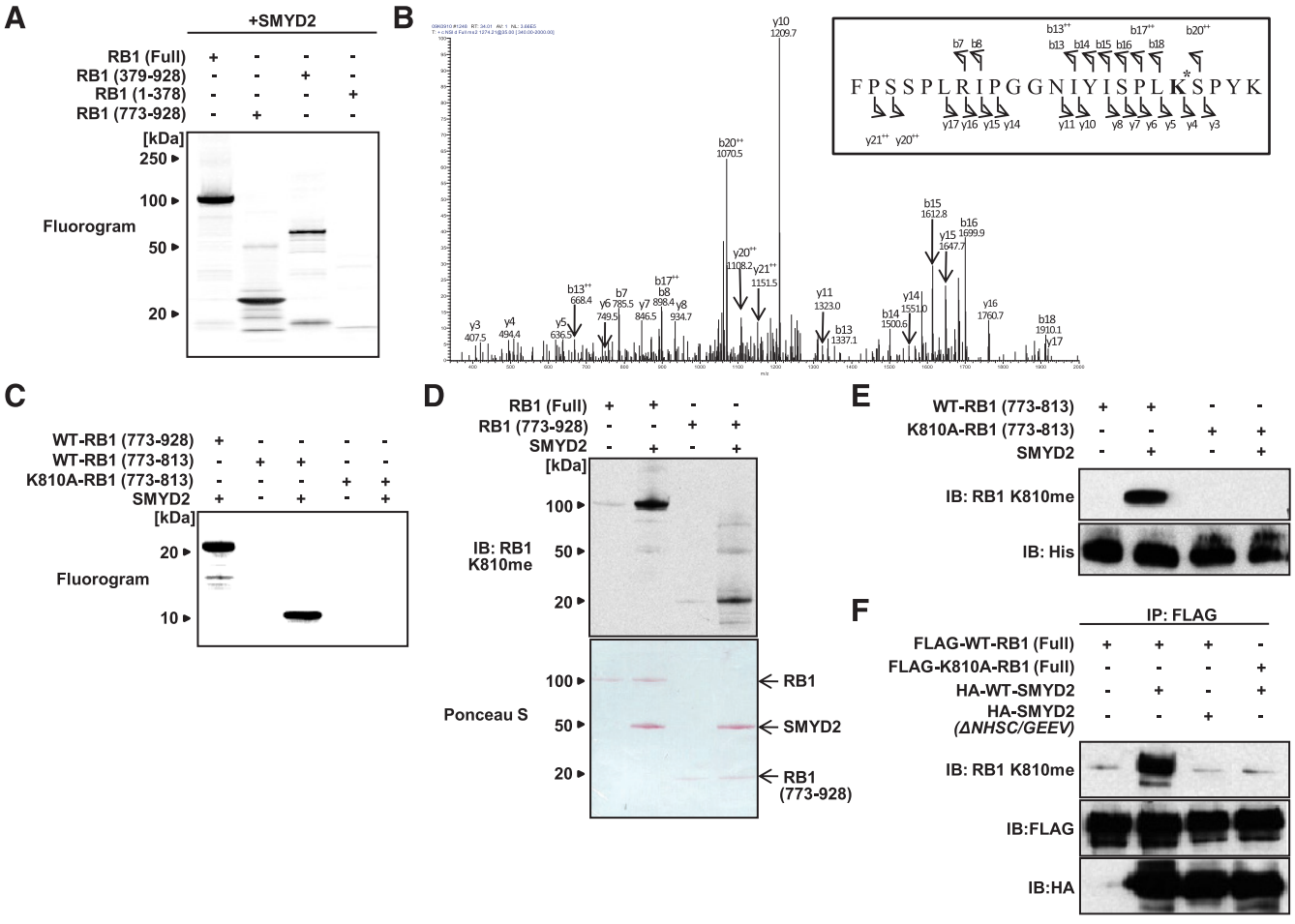

Figure 3. SMYD2 methylates RB1 at K810. (A) The C-terminal region of RB1 is methylated by SMYD2. *In vitro* methyltransferase assay was performed using purified RB1 recombinant proteins (RB1 (Full), RB1 (1-378), RB1 (379-928), and RB1 (773-928)), and methylated proteins were visualized with fluorography. (B) MS/MS spectrum of monomethyl peptide of RB1. RB1 protein (773-928) was treated with SMYD2 and then the mixture was subjected to SDS-PAGE. After CBB staining, a protein band of ~25 kDa was digested with API and subjected to LC-MS/MS. A spectrum for the monomethylated RB1 is shown. The *K indicates monomethyl lysine. (C) K810A-RB1 is not methylated by SMYD2. *In vitro* methyltransferase assay was performed using RB1 (773-928, 773-813), K810A-RB1 (773-813). (D and E) Validation of the anti-K810me RB1 antibody. *In vitro* methyltransferase assay was conducted with RB1 (Full) and RB1 (773-928) (D) or RB1 (773-813) and K810A-RB1 (773-813) (E). The samples were immunoblotted with anti-RB1K810me and anti-His (internal control) antibodies. (F) 293T cells were cotransfected with a FLAG-WT-RB1 vector or a FLAG-K810A-RB1 vector and an HA-WT-SMYD2 vector or an HA-SMYD2 (ΔNHSC/GEEV) vector. Immunoprecipitation was performed using anti-FLAG M2 agarose, and the samples were immunoblotted with anti-RB1K810me, anti-FLAG, and anti-HA antibodies.

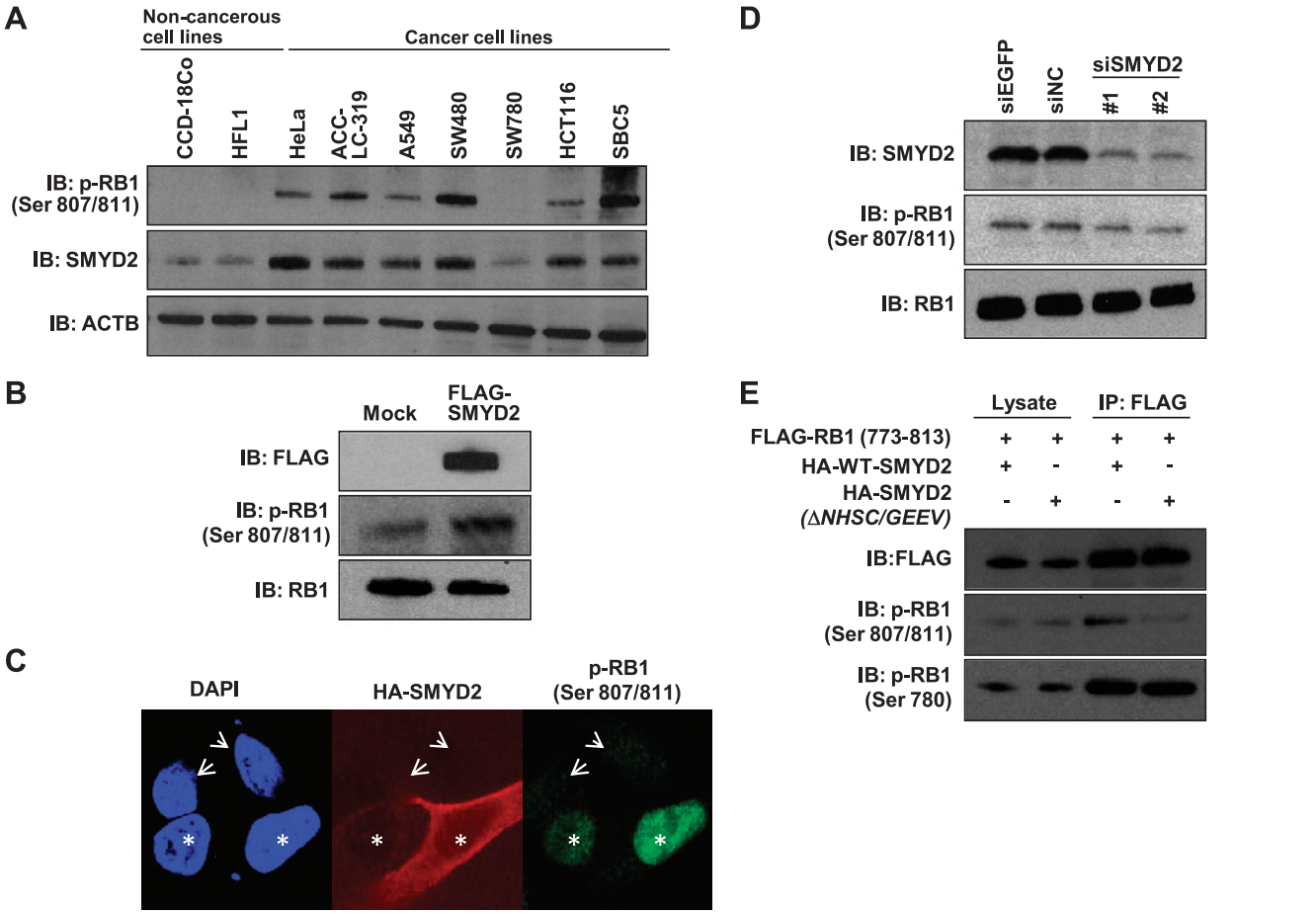

Figure 4. SMYD2 enhances RB1 phosphorylation. (A) Expression levels of SMYD2 correlate with phosphorylation levels of RB1 (Ser 807/811). Lysates from normal cell lines (CCD18Co and HFL1) and cancer cell lines (HeLa, ACC-LC-319, A549, SW480, SW780, HCT116, and SBC5) were immunoblotted with anti–phospho-RB1 (Ser 807/811), anti-SMYD2, and anti-ACTB (internal control) antibodies. (B) 293T cells were transfected with a FLAG-SMYD2 vector and a mock vector (negative control). Cells were lysed with RIPA-like buffer containing complete protease inhibitor cocktail, and samples were immunoblotted with anti-FLAG, anti–phospho-RB1 (Ser 807/811), and anti-RB1 (internal control) antibodies. (C) After transfection with an HA-SMYD2 vector into HeLa cells, cells were fixed with 4% paraformaldehyde (PFA) and permeabilized with 0.5% Triton X-100. The fixed cells were stained with anti–phospho-RB1 (Ser 807/811) (Alexa Fluor 488 [green]) and anti-HA (Alexa Fluor 594 [red]) antibodies, and DAPI (blue). (D) Knockdown of SMYD2 diminishes phosphorylation levels of RB1 (Ser 807/811). After knockdown of SMYD2 using SMYD2-specific siRNAs, cells were lysed with RIPA-like buffer containing complete protease inhibitor cocktail. Immunoblot was performed with anti-SMYD2, anti–phospho-RB1 (Ser 807/811), and anti-RB1 (internal control) antibodies. (E) 293T cells were transfected with a FLAG-RB1 (773-813) vector and an HA-WT-SMYD2 vector and an HA-SMYD2 (ΔNHSC/GEEV) vector. Immunoprecipitation was conducted with anti-FLAG M2 agarose. Anti-FLAG, anti–phospho-RB1 (Ser 807/811), and anti–phospho-RB1 (Ser 780) antibodies were used for immunoblot analysis.

we performed an E2F reporter assay to examine the effect of RB1 methylation on the cell cycle. E2F-luciferase activity was significantly low in the cells overexpressing Lys 810-substituted RB1 compared with the cells overexpressing wild-type RB1 (Figure 6*C*). This result indicated that Lys 810 methylation of RB1 might promote E2F transcriptional activity *in vivo*. Furthermore, we established stable cell lines, which can express wild-type RB1 (WT) and K810-substituted RB1 (K810A) by induction of doxycycline, using Flp-In T-REx 293 cell line system. Consistent with our data, cells expressing wild-type RB1 showed higher cell growth rate than cells expressing RB1 (K810A; Figure W6). Taken together, Lys 810 methylation of RB1 by SMYD2 seems to promote cell cycle progression through an increase in RB1 phosphorylation.

Discussion

The *RB1* gene, a member of the pocket family with *p107* and *p130*, was the first known tumor suppressor [26,27]. The RB protein mainly functions as a transcriptional cofactor that can regulate numerous transcriptional factors and affect the expression of a large number of target genes. In addition, it is well known that the RB1 protein is targeted by the transforming proteins of the DNA tumor viruses like adenoviral E1A and is functionally inactivated in most human tumor cells owing to mutations of either the *RB1* gene itself or its upstream regulators [28]. Its tumor suppressive activity is largely dependent on its ability to directly bind to members of the E2F transcriptional family and prevent them from promoting transcription of genes required for cell proliferation [28]. Researchers have paid attention to the RB/E2F pathway because it is often altered in cancer cells and deregulates the cell proliferation control system [29]. With regard to the cell proliferation regulation, mitogens reverse transcriptional inhibition of E2F-dependent promoters through sequential activation of CDK-cyclin complexes, which phosphorylate RB and attenuate its transcriptional corepressor capability [2,30,31]. This phosphorylation

is sufficient to induce RB protein to release E2F, and subsequently induce the E2F-responsive genes at the late G_1 phase. Importantly, most human tumors carry mutations that disable RB protein-mediated repression of E2F [5]. These mutations either inactivate the *RB1* gene itself or promote phosphorylation of RB protein in the absence of normal mitogenic signal through activation of the cyclin D–CDK4/6 kinases or inactivation of the CDK inhibitor p16. These alterations result in the inappropriate release of E2F, thereby inducing transcriptional activation of E2F target genes and, consequently, enhancing cell proliferation in cancer cells [27]. In this study, we found that Lys 810 of RB1 is monomethylated by SMYD2, which promotes cell cycle progression through elevation of RB1 phosphorylation and E2F1 transcriptional activity (Figure 6*D*). This result adds new insight in the deregulation mechanism of the RB/E2F pathway in human cancer cells. Intriguingly, most recently, other groups also identified lysine methylation on RB protein [32,33]. Taken together, lysine methylation is likely to play a critical role in the regulation of RB functions, and further functional analyses may totally unveil the importance of lysine methylation in the RB/E2F pathway.

We previously showed that some histone methyltransferases (HMTs) play vital roles in human cancer pathogenesis [22,34–36]. Other groups have also proposed involvement of HMTs in malignant alterations of human cells [37–39]. These kinds of evidence clearly indicate that deregulation of HMTs makes a significant contribution to human carcinogenesis, but the detailed molecular mechanisms of HMTs abnormality in human carcinogenesis still remains to be

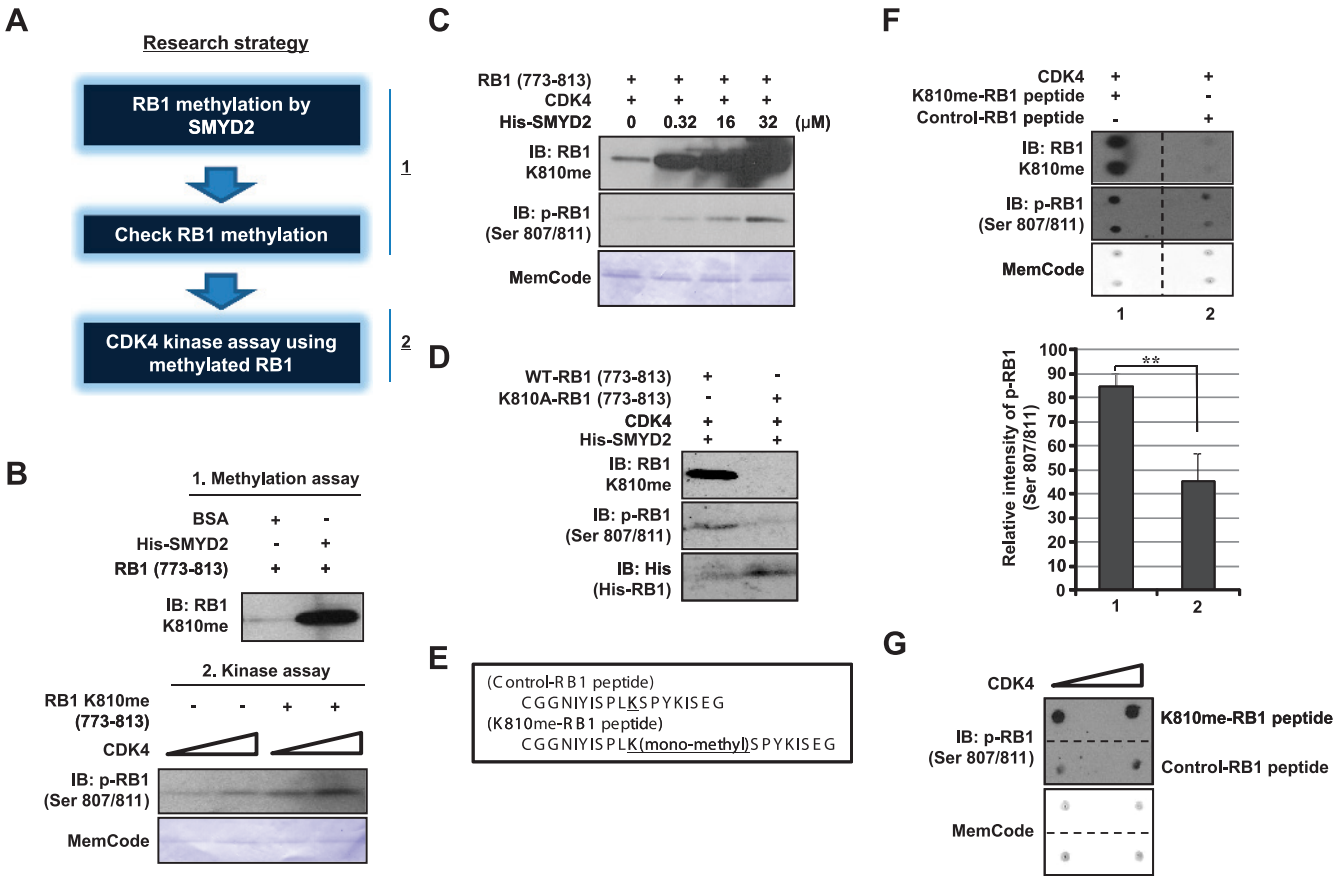

Figure 5. SMYD2-dependent monomethylation of RB1 at Lys 810 increases the phosphorylation of RB1 at Ser 807/811 *in vitro*. (A) Research strategy of sequential *in vitro* methylation and kinase assays. (B) *In vitro* methyltransferase assay was performed using recombinant RB1 (773-813) protein as a substrate reacted with bovine serum albumin (negative control) or SMYD2 as an enzyme. After confirmation of RB1 methylation by Western blot with anti-RB1K810me antibody, *in vitro* kinase assay was conducted using CDK4/Cyclin D1 complex as an enzyme. The samples were immunoblotted with an anti–phospho-RB1 (Ser 807/811) antibody. Amounts of loading proteins were visualized by MemCode Reversible Protein Stain (Thermo Fisher Scientific). (C) Methylation of RB1 at Lys 810 enhances phosphorelation levels of RB1 (Ser 807/811). After *in vitro* methyltransfease assay of RB1 treated with several different doses of SMYD2, *in vitro* kinase assay was performed with CDK4/Cyclin D1 complex as an enzyme. The samples were immunoblotted with anti–phopspho-RB1 (Ser 807/811) and anti-RB1 K810me antibodies. Amounts of loading proteins were visualized by MemCode Reversible Protein Stain (Thermo Fisher Scientific). (D) *In vitro* methyltransferase and kinase assays with WT-RB1 (773-813) and K810A-RB1 (773-813). Anti–RB1 K810me, anti–phospho-RB1 (Ser 807/811), and anti-His (internal control) antibodies were used for the immunoblot analysis. (E) Sequences of methylated and unmethylated peptides of RB1. (F) *In vitro* kinase assay of K810 methylated or unmethylated RB1 peptides was performed with CDK4/Cyclin D1 as an enzyme source. Anti-RB1 K810me and anti–phospho-RB1 (Ser 807/811) antibodies were used for immunoblot analysis. Amounts of loading peptides were visualized by MemCode Reversible Protein Stain (Thermo Fisher Scientific). Mean ± SD (error bars) of two independent experiments. *P* values were calculated using Student's *t* test (**$P < .01$). (G) *In vitro* kinase assay of RB1 peptides treated with two different doses of CDK4/Cyclin D1. Amounts of loading peptides were visualized by MemCode Reversible Protein Stain (Thermo Fisher Scientific).

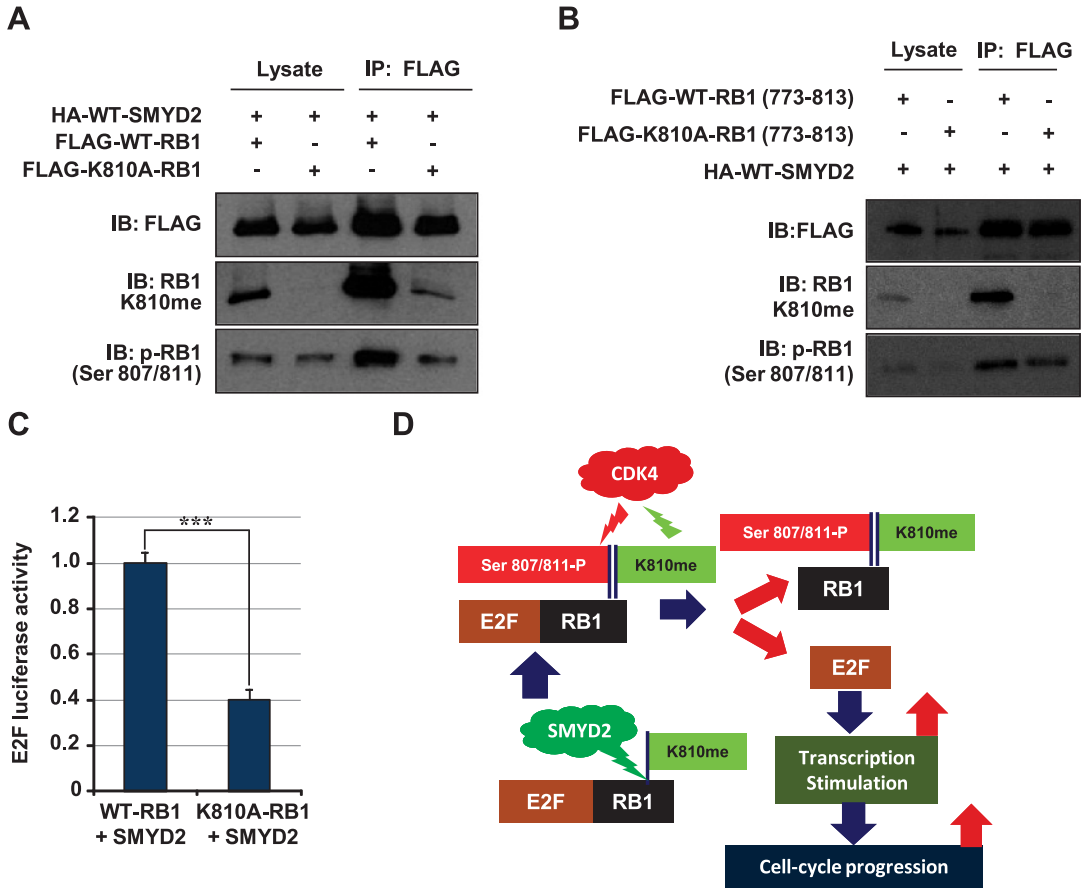

Figure 6. Lys 810 methylation of RB1 enhances the phosphorylation of RB1 and E2F luciferase activity *in vivo*. (A) 293T cells were transfected with a HA-WT-SMYD2 vector and a FLAG-WT-RB1 vector or a FLAG-K810A-RB1 vector. Immunoprecipitation was conducted with anti–FLAG M2 agarose. Anti-FLAG, anti-RB1 K810me, and anti–phospho-RB1 (Ser 807/811) antibodies were used for immunoblot analysis. (B) 293T cells were transfected with a FLAG-WT-RB1 (773-813) vector or a FLAG-K810A-RB1 (773-813) vector and a HA-WT-SMYD2 vector. Immunoprecipitation was conducted with anti–FLAG M2 agarose. Anti-FLAG, anti-RB1 K810me, and anti–phospho-RB1 (Ser 807/811) antibodies were used for immunoblot analysis. (C) E2F reporter assay after overexpression of WT-RB1 and K810A-RB1 in 293T cells. Mean ± SD (error bars) of three independent experiments. *P* values were calculated using Student's *t* test (***$P < .001$). (D) A schematic model for the dynamic regulation of RB1 phosphorylation through methylation of RB1 by SMYD2.

clarified. In this study, we demonstrated that SMYD2 is overexpressed in various cancer tissues and that SMYD2 methylates RB1 as a substrate. Although some novel targets have been identified and newly emerging anticancer drugs are under clinical trials, current chemotherapy fails to ensure satisfying outcomes, and adverse events are still not negligible [40,41]. Therefore, it is crucial to identify ideal therapeutic targets to improve the efficacy and decrease the adverse effects for providing the better quality lives to cancer patients. According to our study, SMYD2 plays a crucial role in human carcinogenesis. Importantly, Komatsu et al. [42] recently revealed that overexpression of SMYD2 protein was frequently detected in primary tumor samples of esophageal squamous cell carcinoma, and patients with SMYD2-overexpressing tumors had worse overall rate of survival than those with nonexpressing tumors. In addition, SMYD2 positivity was independently associated with a worse outcome in the multivariate analysis [42]. Taken together, considering that methodologies to generate HMTs inhibitors have recently been developed [43,44], SMYD2 is likely to be an ideal therapeutic target in cancer, with fewer adverse events because of its low expression in normal cells. Further study may reinforce the importance of SMYD2 as a target of cancer therapy, and the development of a SMYD2 specific inhibitor seems to be one of the promising strategies of cancer therapy.

Acknowledgments

The authors thank Noriko Ikawa, Haruka Sawada, and Yukiko Iwai for technical assistance.

References

[1] Burkhart DL and Sage J (2008). Cellular mechanisms of tumour suppression by the retinoblastoma gene. *Nat Rev Cancer* **8**, 671–682.
[2] Knudsen ES and Knudsen KE (2008). Tailoring to RB: tumour suppressor status and therapeutic response. *Nat Rev Cancer* **8**, 714–724.
[3] Weinberg RA (1995). The retinoblastoma protein and cell cycle control. *Cell* **81**, 323–330.
[4] Sherr CJ (1996). Cancer cell cycles. *Science* **274**, 1672–1677.
[5] Sherr CJ and McCormick F (2002). The RB and p53 pathways in cancer. *Cancer Cell* **2**, 103–112.
[6] Chan HM, Krstic-Demonacos M, Smith L, Demonacos C, and La Thangue NB (2001). Acetylation control of the retinoblastoma tumour-suppressor protein. *Nat Cell Biol* **3**, 667–674.

[7] Nguyen DX, Baglia LA, Huang SM, Baker CM, and McCance DJ (2004). Acetylation regulates the differentiation-specific functions of the retinoblastoma protein. *EMBO J* **23**, 1609–1618.

[8] Pickard A, Wong PP, and McCance DJ (2010). Acetylation of Rb by PCAF is required for nuclear localization and keratinocyte differentiation. *J Cell Sci* **123**, 3718–3726.

[9] Brown MA, Sims RJ III, Gottlieb PD, and Tucker PW (2006). Identification and characterization of Smyd2: a split SET/MYND domain-containing histone H_3 lysine 36-specific methyltransferase that interacts with the Sin3 histone deacetylase complex. *Mol Cancer* **5**, 26.

[10] Huang J, Perez-Burgos L, Placek BJ, Sengupta R, Richter M, Dorsey JA, Kubicek S, Opravil S, Jenuwein T, and Berger SL (2006). Repression of p53 activity by Smyd2-mediated methylation. *Nature* **444**, 629–632.

[11] Kawamura S, Yoshigai E, Kuhara S, and Tashiro K (2008). Smyd1 and Smyd2 are expressed in muscle tissue in *Xenopus laevis*. *Cytotechnology* **57**, 161–168.

[12] Diehl F, Brown MA, van Amerongen MJ, Novoyatleva T, Wietelmann A, Harriss J, Ferrazzi F, Bottger T, Harvey RP, Tucker PW, et al. (2010). Cardiac deletion of Smyd2 is dispensable for mouse heart development. *PLoS One* **5**, e9748.

[13] Gottlieb PD, Pierce SA, Sims RJ, Yamagishi H, Weihe EK, Harriss JV, Maika SD, Kuziel WA, King HL, Olson EN, et al. (2002). Bop encodes a muscle-restricted protein containing MYND and SET domains and is essential for cardiac differentiation and morphogenesis. *Nat Genet* **31**, 25–32.

[14] Cho HS, Kelly JD, Hayami S, Toyokawa G, Takawa M, Yoshimatsu M, Tsunoda T, Field HI, Neal DE, Ponder BA, et al. (2011). Enhanced expression of EHMT2 is involved in the proliferation of cancer cells through negative regulation of SIAH1. *Neoplasia* **13**, 676–684.

[15] Cho HS, Toyokawa G, Daigo Y, Hayami S, Masuda K, Ikawa N, Yamane Y, Maejima K, Tsunoda T, Field HI, et al. (2011). The JmjC domain-containing histone demethylase KDM3A is a positive regulator of the G(1) /S transition in cancer cells via transcriptional regulation of the *HOXA1* gene. *Int J Cancer*, E-pub ahead of print.

[16] Hayami S, Kelly JD, Cho HS, Yoshimatsu M, Unoki M, Tsunoda T, Field HI, Neal DE, Yamaue H, Ponder BA, et al. (2011). Overexpression of LSD1 contributes to human carcinogenesis through chromatin regulation in various cancers. *Int J Cancer* **128**, 574–586.

[17] Hayami S, Yoshimatsu M, Veerakumarasivam A, Unoki M, Iwai Y, Tsunoda T, Field HI, Kelly JD, Neal DE, Yamaue H, et al. (2010). Overexpression of the JmjC histone demethylase KDM5B in human carcinogenesis: involvement in the proliferation of cancer cells through the E2F/RB pathway. *Mol Cancer* **9**, 59.

[18] Toyokawa G, Cho HS, Iwai Y, Yoshimatsu M, Takawa M, Hayami S, Maejima K, Shimizu N, Tanaka H, Tsunoda T, et al. (2011). The histone demethylase JMJD2B plays an essential role in human carcinogenesis through positive regulation of cyclin-dependent kinase 6. *Cancer Prev Res (Phila)* **4**, 2051–2061.

[19] Toyokawa G, Cho HS, Masuda K, Yamane Y, Yoshimatsu M, Hayami S, Takawa M, Iwai Y, Daigo Y, Tsuchiya E, et al. (2011). Histone lysine methyltransferase Wolf-Hirschhorn syndrome candidate 1 is involved in human carcinogenesis through regulation of the Wnt pathway. *Neoplasia* **13**, 887–898.

[20] Toyokawa G, Masuda K, Daigo Y, Cho HS, Yoshimatsu M, Takawa M, Hayami S, Maejima K, Chino M, Field HI, et al. (2011). Minichromosome maintenance protein 7 is a potential therapeutic target in human cancer and a novel prognostic marker of non–small cell lung cancer. *Mol Cancer* **10**, 65.

[21] Olsburgh J, Harnden P, Weeks R, Smith B, Joyce A, Hall G, Poulsom R, Selby P, and Southgate J (2003). Uroplakin gene expression in normal human tissues and locally advanced bladder cancer. *J Pathol* **199**, 41–49.

[22] Yoshimatsu M, Toyokawa G, Hayami S, Unoki M, Tsunoda T, Field HI, Kelly JD, Neal DE, Maehara Y, Ponder BA, et al. (2011). Dysregulation of PRMT1 and PRMT6, type I arginine methyltransferases, is involved in various types of human cancers. *Int J Cancer* **128**, 562–573.

[23] Masaki T, Tanabe M, Nakamura K, and Soejima M (1981). Studies on a new proteolytic enzyme from Achromobacter lyticus M497-1. I. Purification and some enzymatic properties. *Biochim Biophys Acta* **660**, 44–50.

[24] Masuda A and Dohmae N (2010). Automated protein hydrolysis delivering sample to a solid acid catalyst for amino acid analysis. *Anal Chem* **82**, 8939–8945.

[25] Cho HS, Suzuki T, Dohmae N, Hayami S, Unoki M, Yoshimatsu M, Toyokawa G, Takawa M, Chen T, Kurash JK, et al. (2011). Demethylation of RB regulator MYPT1 by histone demethylase LSD1 promotes cell cycle progression in cancer cells. *Cancer Res* **71**, 1–6.

[26] Friend SH, Bernards R, Rogelj S, Weinberg RA, Rapaport JM, Albert DM, and Dryja TP (1986). A human DNA segment with properties of the gene that predisposes to retinoblastoma and osteosarcoma. *Nature* **323**, 643–646.

[27] Ianari A, Natale T, Calo E, Ferretti E, Alesse E, Screpanti I, Haigis K, Gulino A, and Lees JA (2009). Proapoptotic function of the retinoblastoma tumor suppressor protein. *Cancer Cell* **15**, 184–194.

[28] Trimarchi JM and Lees JA (2002). Sibling rivalry in the E2F family. *Nat Rev Mol Cell Biol* **3**, 11–20.

[29] Knudsen ES and Wang JY (2010). Targeting the RB-pathway in cancer therapy. *Clin Cancer Res* **16**, 1094–1099.

[30] Harbour JW, Luo RX, Dei Santi A, Postigo AA, and Dean DC (1999). Cdk phosphorylation triggers sequential intramolecular interactions that progressively block Rb functions as cells move through G_1. *Cell* **98**, 859–869.

[31] Hinds PW, Mittnacht S, Dulic V, Arnold A, Reed SI, and Weinberg RA (1992). Regulation of retinoblastoma protein functions by ectopic expression of human cyclins. *Cell* **70**, 993–1006.

[32] Carr SM, Munro S, Kessler B, Oppermann U, and La Thangue NB (2011). Interplay between lysine methylation and Cdk phosphorylation in growth control by the retinoblastoma protein. *EMBO J* **30**, 317–327.

[33] Saddic LA, West LE, Aslanian A, Yates JR III, Rubin SM, Gozani O, and Sage J (2010). Methylation of the retinoblastoma tumor suppressor by SMYD2. *J Biol Chem* **285**, 37733–37740.

[34] Hamamoto R, Furukawa Y, Morita M, Iimura Y, Silva FP, Li M, Yagyu R, and Nakamura Y (2004). SMYD3 encodes a histone methyltransferase involved in the proliferation of cancer cells. *Nat Cell Biol* **6**, 731–740.

[35] Hamamoto R, Silva FP, Tsuge M, Nishidate T, Katagiri T, Nakamura Y, and Furukawa Y (2006). Enhanced SMYD3 expression is essential for the growth of breast cancer cells. *Cancer Sci* **97**, 113–118.

[36] Takawa M, Masuda K, Kunizaki M, Daigo Y, Takagi K, Iwai Y, Cho HS, Toyokawa G, Yamane Y, Maejima K, et al. (2011). Validation of the histone methyltransferase EZH2 as a therapeutic target for various types of human cancer and as a prognostic marker. *Cancer Sci* **102**, 1298–1305.

[37] Portela A and Esteller M (2010). Epigenetic modifications and human disease. *Nat Biotechnol* **28**, 1057–1068.

[38] Schneider R, Bannister AJ, and Kouzarides T (2002). Unsafe SETs: histone lysine methyltransferases and cancer. *Trends Biochem Sci* **27**, 396–402.

[39] Sparmann A and van Lohuizen M (2006). Polycomb silencers control cell fate, development and cancer. *Nat Rev Cancer* **6**, 846–856.

[40] Black PC, Agarwal PK, and Dinney CP (2007). Targeted therapies in bladder cancer—an update. *Urol Oncol* **25**, 433–438.

[41] Sonpavde G, Sternberg CN, Rosenberg JE, Hahn NM, Galsky MD, and Vogelzang NJ (2010). Second-line systemic therapy and emerging drugs for metastatic transitional-cell carcinoma of the urothelium. *Lancet Oncol* **11**, 861–870.

[42] Komatsu S, Imoto I, Tsuda H, Kozaki KI, Muramatsu T, Shimada Y, Aiko S, Yoshizumi Y, Ichikawa D, Otsuji E, et al. (2009). Overexpression of SMYD2 relates to tumor cell proliferation and malignant outcome of esophageal squamous cell carcinoma. *Carcinogenesis* **30**, 1139–1146.

[43] Copeland RA, Solomon ME, and Richon VM (2009). Protein methyltransferases as a target class for drug discovery. *Nat Rev Drug Discov* **8**, 724–732.

[44] Spannhoff A, Heinke R, Bauer I, Trojer P, Metzger E, Gust R, Schule R, Brosch G, Sippl W, and Jung M (2007). Target-based approach to inhibitors of histone arginine methyltransferases. *J Med Chem* **50**, 2319–2325.

Table W1. Primer Sequences for Quantitative RT-PCR.

Gene	Name	Primer Sequence
GAPDH (housekeeping gene)	GAPDH-f	GCAAATTCCATGGCACCGTC
	GAPDH-r	TCGCCCCACTTGATTTTGG
SDH (housekeeping gene)	SDH-f	TGGGAACAAGAGGGCATCTG
	SDH-r	CCACCACTGCATCAAATTCATG
SMYD2	SMYD2-f	ATCTCCTGTACCCAACGGAAG
	SMYD2-r	CACCTTGGCCTTATCCTTGTCC

Table W2. siRNA Sequences.

siRNA Name	Sequence	
siEGFP	Sense	GCAGCACGACUUCUUCAAG
	Antisense	CUUGAAGAAGUCGUGCUGC
siNegative control (cocktail)		
Target no. 1	Sense	AUCCGCGCGAUAGUACGUA
	Antisense	UACGUACUAUCGCGCGGAU
Target no. 2	Sense	UUACGCGUAGCGUAAUACG
	Antisense	CGUAUUACGCUACGCGUAA
Target no. 3	Sense	UAUUCGCGCGUAUAGCGGU
	Antisense	ACCGCUAUACGCGCGAAUA
siSMYD2 no. 1	Sense	GAUUUGAUUCAGAGUGACA
	Antisense	UGUCACUCUGAAUCAAAUC
siSMYD2 no. 2	Sense	GAAUGACCGGUUAAGAGA
	Antisense	UCUCUUAACCGGUCAUUUC

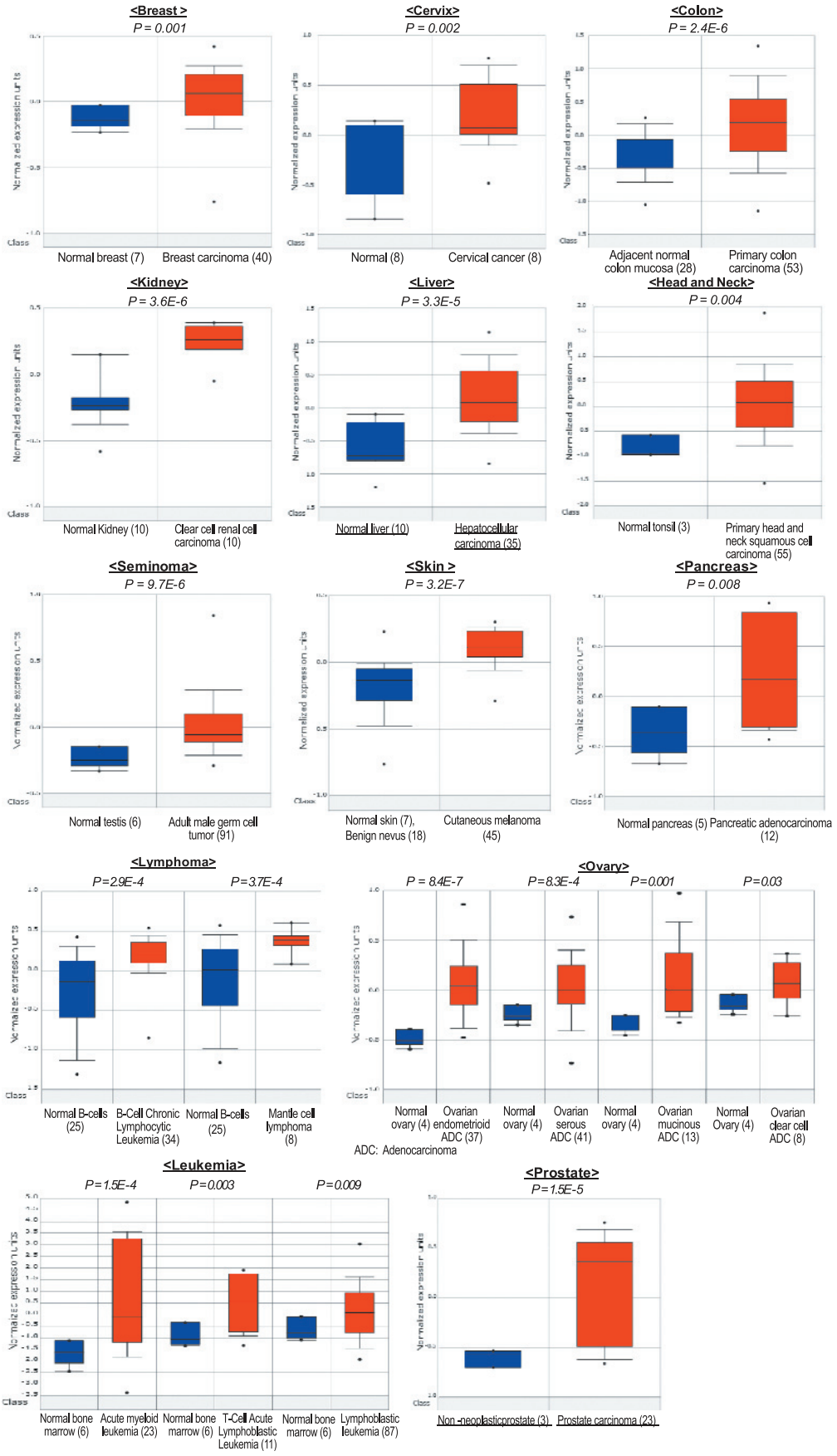

Figure W1. SMYD2 is overexpressed in various types of cancer. Gene expression data in Oncomine was analyzed. The thick bars in the boxes are average expression levels, and the boxes represent 95% of the samples. The error bars are above or below the boxes, and the range of expression levels is enclosed by two dots.

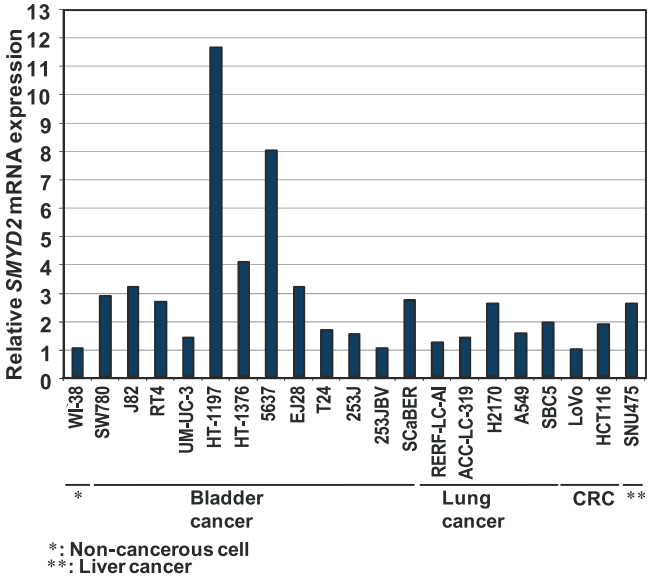

Figure W2. Quantitative RT-PCR analysis was performed to examine expression levels of SMYD2 at the mRNA level in two non-cancerous cell lines (WI-38 and IMR-90), 14 bladder cancer cell lines (SW780, J82, RT4, UMUC3, HT-1197, HT-1376, 5637, EJ28, T24, 253J, 253JBV, and SCaBER), 5 lung cancer cell lines (RERF-LC-AI, ACC-LC-319, H2170, A549, and SBC5), 2 colon cancer cell lines (LoVo and HCT116), and 1 liver cancer cell line (SNU475).

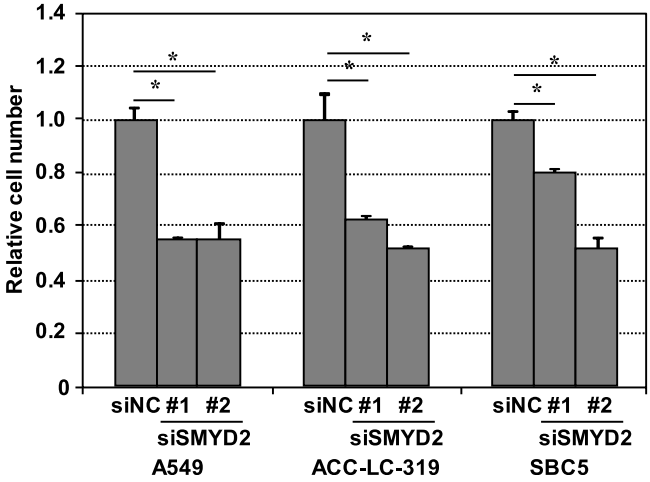

Figure W3. Effects of SMYD2 knockdown on the proliferation of lung cancer cell lines. Relative cell numbers are measured by Cell Counting Kit-8 and normalized to the number of siNC-treated cells (siNC = 1): results are the mean ± SD (error bars) of three independent experiments. *P* values were calculated using Student's *t* test (*$P < .05$).

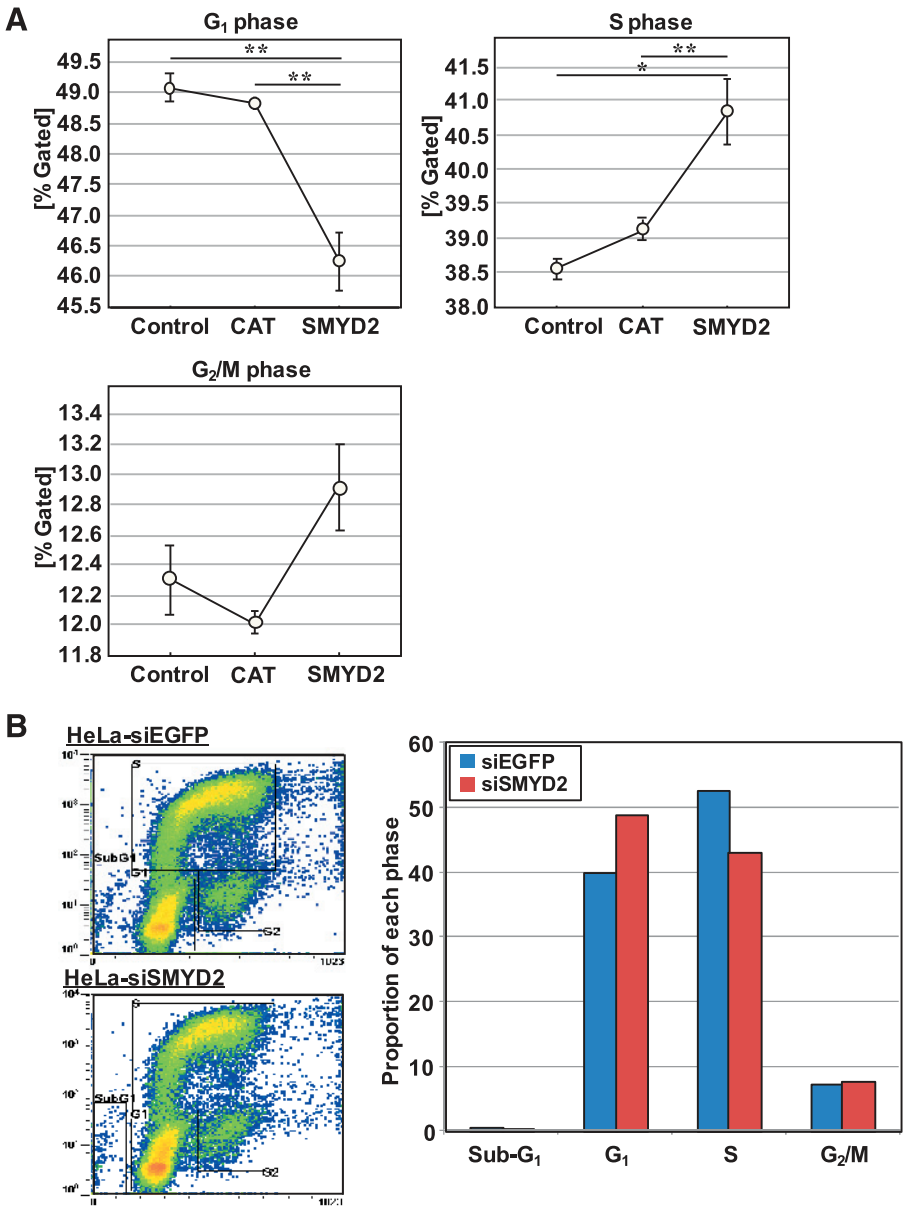

Figure W4. SMYD2 promotes the G_1/S transition of cell cycle. (A) Numerical analysis of the FACS result, classifying cells by cell cycle status. The proportion of T-REx-SMYD2 cells in S phases is slightly higher than control cells (T-REx-Mock and T-REx-CAT). Mean ± SD (error bars) of three independent experiments. Fisher Protected least significant difference *post hoc* test was used to calculate *P* values (**$P < .01$, *$P < .05$). (B) Cell cycle distribution was analyzed by flow cytometry after coupled staining with fluorescein isothiocyanate–conjugated anti-BrdU and 7-amino-actinomycin D as described in Materials and Methods.

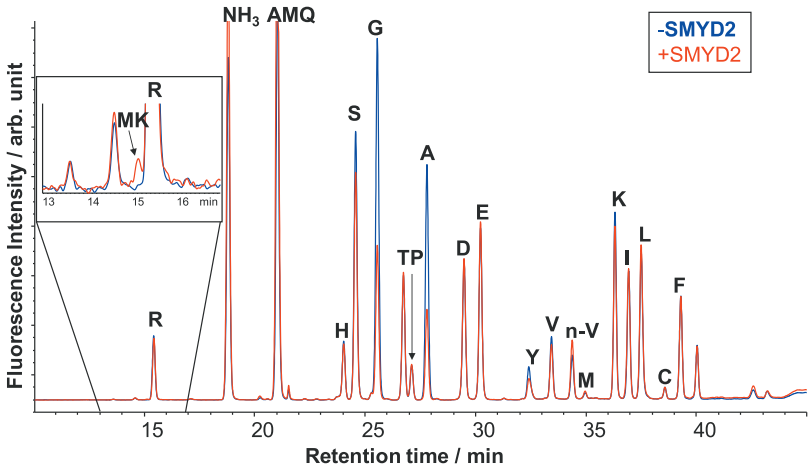

Figure W5. Chromatogram of amino acids obtained by acid hydrolysis of RB1 after treatment with SMYD2 (red line) or without SMYD2 (blue line). Inserted figure shows a magnified view of the region around the arginine. Except for monomethylated lysine (MK) and norvaline (n-V), amino acid residues are annotated using their one-letter abbreviations. AMQ indicates 6-amino quinoline derived from hydrolysis of the derivatizing reagent for amino acids; NH_3, ammonia.

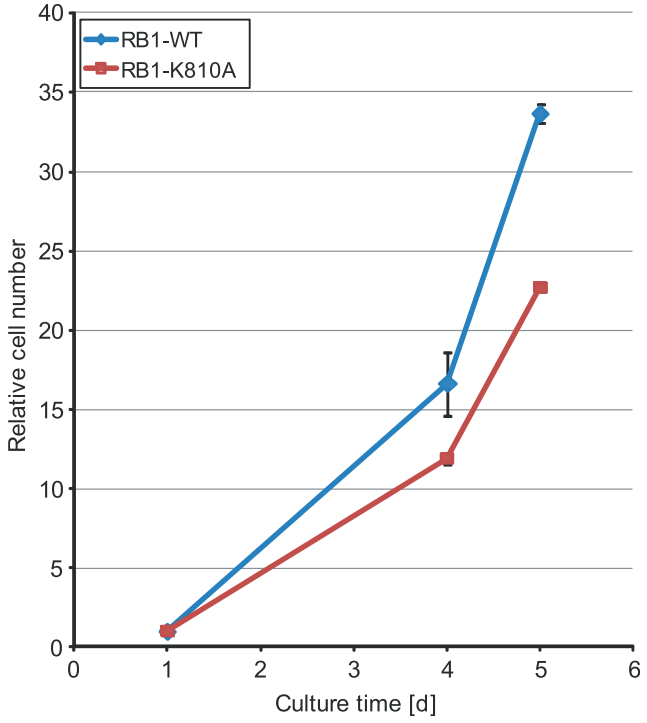

Figure W6. Cell growth analysis of Flp-In T-REx 293 cell lines. We established stable cell lines, which can overexpress wild-type RB1 (RB1-WT) and K810-substituted RB1 (RB1-K810A), using Flp-IN T-REx system (Life Technologies). Both wild-type and K810-substituted RB1 proteins were induced by 1 μg/ml doxycycline. The number of cells were calculated by Cell Counting Kit-8 (Dojindo, Kumamoto, Japan), and the y value shows the relative cell number to day 1 ($d_1 = 1$).